Analyst

Accepted Manuscript

This article can be cited before page numbers have been issued, to do this please use: Y. Liu, Z. Zhu, C. Wang, R. Gao, X. yang and S. Liu, *Analyst*, 2019, DOI: 10.1039/C8AN02313A.

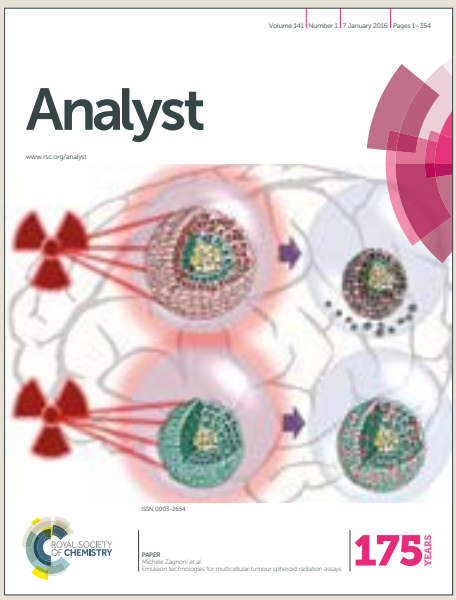

Analyst

View Article Online
DOI: 10.1039/C8AN02313A

ARTICLE

Responsive surface bioaffinity binding to construct flexible and sensitive electrochemical aptasensor

Received 00th January 20xx,
Accepted 00th January 20xx

DOI: 10.1039/x0xx00000x

www.rsc.org/

Ying Liu, Zhencai Zhu, Chao Wang, Rui Gao, Xiaoyan Yang, and Shufeng Liu*

Development of simple, flexible, cost-effective and sensitive electrochemical biosensing strategies is highly desirable to advance the applications in disease diagnostics and clinical biomedicine. Herein, we fabricated a new enzyme-based electrochemical aptasensor with the use of adenosine triphosphate (ATP) and thrombin as model targets on the basis of a responsive surface bioaffinity binding strategy. It took full advantages of an immobilized complex duplex probe (hybrids of a hairpin-like aptamer probe with a digoxigenin (Dig)-labeled immobilization strand) to effectively inhibit the approaching of bulky horseradish peroxidase linked-anti-Dig antibody (anti-Dig-HRP) to the Dig on the electrode due to the steric effect. The target recognition dissociated the aptamer strand from the duplex probe and exposed the Dig for its effective binding with anti-Dig-HRP. The successive electrocatalysis offered a significantly amplified electrochemical signal correlated with target recognition event. Sensitive detection toward ATP and thrombin was achieved with detection limits of 0.87 nM and 6.3 pM, respectively. The proposed strategy is simple and sensitive without complex operation that confronts many amplified aptasensors. Also, the target recognition and signal reporting units are relatively isolated, making the biosensor fabrication more flexible. It thus provided a new and versatile pathway for sensitive biosensor fabrication.

Introduction

Aptamers are single-stranded DNA or RNA molecules selected from random sequence nucleic acid libraries by an in vitro selection technique called SELEX.[1-3] They can specifically bind to a wide range of targets from small molecules, metal ions, proteins, cells to viruses.[4-7] Aptamer exhibits some intrinsic advantages such as simple synthesis, easy labelling, robust stability and applications, rendering it as one of most importantly biological recognition elements.[8,9] Accompanied with the advance of aptamer screening technique, more and more aptamers toward a wide range of target molecules are exploited. Thus, the development of aptamer-based analysis method with the advantages of simplicity, low cost, adaptability and high sensitivity is highly demanded to accommodate the wide applications in disease diagnostics, biomarker discovery and clinical biomedicine research. Up until now various methods including electrochemistry, fluorescence, colorimetry, photoelectrochemistry, electroluminescence, surface enhanced raman scattering, surface plasmon resonance, quartz crystal microbalance, have been widely employed for aptasensor fabrication.[10-16]

Electrochemical method is especially attractive for aptasensor fabrication owing to its simple instrumentation, high sensitivity, operational flexibility, and ease of miniaturization and integration.[17-20] The typical electrochemical aptamer-based sensors are usually based on the target-induced conformational change of aptamer, which induces the coupled redox moiety distant or approaching from electrode surface to achieve a signal-off or -on output.[21-23] For example, Fan et al developed a target-responsive electrochemical aptamer switch for ATP detection.[24] The ATP recognition with its aptamer sequence denatured the immobilized duplex DNA (aptamer and its complementary DNA) on the electrode to liberate the complementary DNA into the solution, accompanied with the structural switch from the duplex to the tertiary aptamer structure on the electrode. Thus, the ferrocene moiety labeled onto the aptamer approached the electrode surface to generate measurable electrochemical signals. Mao et al used aptamer-complementary DNA oligonucleotide as probe to fabricate aptamer-based electrochemical sensors.[25] Upon target binding, the aptamers dissociated from their respective complementary DNA (which was immobilized on the electrode and labeled by a redox moiety) into the solution. Thus the single-stranded complementary DNA on the electrode could form a hairpin structure through the hybridization of the complementary sequences at both ends, leading to the signal change of the redox moiety labeled onto the complementary DNA for target sensing. Even though these aptasensor designs are simple and even reagentless, the detection sensitivity

[a] Key Laboratory of Optic-electric Sensing and Analytical Chemistry for Life Science, Ministry of Education, College of Chemistry and Molecular Engineering, Qingdao University of Science and Technology, 53 Zhengzhou Road, Qingdao 266042, China. E-mail: sliu@qust.edu.cn

Electronic Supplementary Information (ESI) available: [Synthesized nucleic acid sequences (Table S1); additional experimental characterizations (Figure S1-S3); detection performance comparison (Table S2-S4)]. See DOI: 10.1039/x0xx00000x

View Article Online DOI: 10.1039/C8AN02717A

needs to be further improved. To further enhance the detection performance, much efforts has also been directed to explore suitable signal amplification strategies. Among them, nanomaterial or DNA-based signal amplification strategies are more often employed.[26-28] For example, Wang et al developed a sensitive electrochemical aptasensor for the simultaneous detection of thrombin and ATP based on DNA structural switching on gold nanoparticles-decorated MoS_2 nanosheets.[29] Chen et al fabricated a sensitive and label-free electrochemical aptasensor for ATP detection by using the DNA-functionalized gold nanoparticles as signal carrier ($[Ru(NH_3)_6]^{3+}$ binding) for signal amplification.[30] But the synthesis, purification and even modification of nanomaterial increases the assay complexity. Since the aptamer could be easily programmed into different nucleic acid structure or nucleic acid hybrids, DNA-based signal amplification such as nuclease-based or enzyme-free nucleic acid assembly strategies is thus very attractive for sensitive aptasensor fabrication.[31-33] For example, Xiang et al demonstrated an aptamer/protein proximity binding-triggered molecular machine approach for sensitive determination of thrombin. The DNA-fueled toehold-mediated strand displacement reaction strategy was employed for signal amplification.[34] Lei et al introduced a binding-induced DNA walker-assisted signal amplification strategy for highly sensitive electrochemical detection of protein.[35] However, they are sometimes still confronted with the relatively complex operation procedures or reagent-intensive processes, or even false-positive output, limiting their wide applications. Therefore, the design of simple, flexible and sensitive electrochemical aptasensor still remains a challenging task.

Herein, we proposed a new and simple enzyme-based electrochemical aptasensor based on a responsive surface bioaffinity binding strategy with the use of ATP and thrombin as model analytes. A complex duplex DNA probe was firstly designed by hybridizing of a hairpin-like aptamer probe with an immobilization strand dually labeled by digoxigenin (Dig) and thiol. The immobilized duplex DNA probe on the electrode could shield the affinity binding of the coupled Dig with the bulky horseradish peroxidase linked-anti-Dig antibody (anti-Dig-HRP) due to the steric effect.[36,37] The target recognition induced the dissociation of aptamer strand from the duplex DNA probe and exposed the Dig for the successive binding with anti-Dig-HRP. Its electrocatalysis toward H_2O_2 in the presence of 3,3',5,5'-tetramethylbenzidine (TMB) as a cosubstrate induced an amplified electrochemical signal related with target recognition event.

Experimental Section

Materials and chemicals

6-Mercapto-1-hexanol (MCH), hexaammineruthenium(III) chloride ($Ru(NH_3)_6^{3+}$), 3,3',5,5'-Tetramethylbenzidinedihydrochloride (TMB), thrombin (from human plasma lyophilized powder, ≥2,000 NIH units/mg protein) and mouse immunoglobin G (IgG) were purchased from Sigma-Aldrich (St. Louis, MO, USA). Anti-Dig-HRP was purchased from Jackson ImmunoResearch Laboratories, Inc. (West Grove, PA, USA). Streptavidin and bovine serum albumin (BSA) were purchased from Dingguo Biotech Co., Ltd. (Beijing, China). Tris(2-carboxyethyl) phosphine hydrochloride (TCEP), fetal calf serum(FBS), adenosine triphosphate (ATP), guanosine triphosphate (GTP), cytidine triphosphate (CTP) and thymidine triphosphate (TTP) were purchased from Sangon Biotech Co., Ltd. (Shanghai, China). NTP was obtained by mixing the same concentration of ATP, GTP, CTP and TTP. The HPLC-purified oligonucleotides were synthesized by Sangon Biotech. Co., Ltd. (Shanghai, China) with the sequences listed in Table S1. All other reagents were of analytical grade without further purification. All solutions were prepared with ultrapure water obtained from a Milli-Q water purification system (Millipore Corp., Bedford, MA, USA) with a resistivity of 18.2 MΩ cm.

Duplex DNA probe modification on the electrode

The gold (2 mm) electrodes were first polished on a microcloth with different alumina suspensions (0.3 and 0.05 mm), and then ultrasonically treated in ethanol and water to remove the residual alumina powder. Then, the electrodes were electrochemically cleaned in a 0.5 M H_2SO_4 solution within a potential window between -0.2 and +1.5 V at a scan rate of 100 mV/s until a stable cyclic voltammogram was obtained. Prior to immobilization on the electrode, the duplex DNA probe was first obtained by mixing the same concentration of hairpin-like aptamer probe (HP) and immobilization probe strand (IP) in 10 μM Tris-HCl buffer (pH 7.4, 0.1 M NaCl), which was then heated to 90 °C for 5 min and allowed to cool to room temperature.[24,38] Such DNA denaturation and renaturation operation could facilitate the formation of duplex DNA probe with the stable secondary structure and avoid any possible undesired DNA structures. Then, TCEP (10 mM) was added to the above mixed solution for 1 hr to reduce the formation of disulfide bonds.[39] The immobilization of duplex DNA probe was operated by incubating the above treated electrode into 50 μL of duplex DNA probe solution for overnight at room temperature. The electrode was then rinsed with 20 mM Tris-HCl buffer solution (0.1 M NaCl, pH 7.4) and dried with nitrogen. The immobilized electrode was afterwards treated with 1 mM MCH solution for 1 hr to remove the non-specifically adsorbed DNA.[40] Finally, the electrode was thoroughly rinsed with a 20 mM Tris-HCl buffer solution (0.1 M NaCl, pH 7.4) and dried with nitrogen before use.

Target detection

The ATP recognition was conducted by incubating the duplex DNA probe modified electrode into 50 μL of different concentrations of ATP solution (10 mM PBS, 100 mM NaCl) at 37 °C for 3 h. After that, the electrode was treated with 2% BSA, and then dropped with 5 μL of anti-Dig-HRP (0.8 μM) for 30 min. Herein, the BSA treatment was used to eliminate the possible non-specific adsorption of anti-Dig-HRP on the electrode to a large extent. Thus, the aroused electrocatalytic signal could be well assigned to the affinity binding of the anti-Dig-HRP with the exposed Dig after ATP recognition. Then the obtained electrode was ready for electrochemical

View Article Online
DOI: 10.1039/C8AN02313A

measurement. The above operation procedures were also applicable for thrombin analysis.

Electrochemical measurements

All electrochemical experiments were performed using a CHI 660E electrochemical workstation (Shanghai Chenhua Instrument Factory) with a three-electrode system (working electrode: 2 mm gold electrode; reference electrode: Ag/AgCl electrode; counter electrode: platinum wire). Amperometric detection was conducted at 0.15 V for 100 s in 0.1 M acetic acid/sodium acetate buffer (pH 5.5, HAc-NaAc) containing 1 mM TMB and 5 mM H_2O_2. It offers a direct way to characterize the HRP catalyzed electrochemical process for sensing performance. Cyclic voltammetry characterization was operated with a scanning potential of 0~0.8 V and a scan rate of 100 mV/s. It was measured into the same testing solution with the amperometric method and could demonstrate the detailed information about the redox process of the HRP-catalyzed TMB and H_2O_2 reaction. Electrochemical impedance spectroscopy (EIS) was performed in 5 mM $[Fe(CN)_6]^{3-/4-}$ (10 mM PBS, pH 7.4, 1 M KCl) with a scan frequency of 0.1 Hz to 10 KHz and an amplitude of 5 mV. It was conducted herein to mainly follow the biosensor fabrication process. The chronocoulometric plots of the duplex DNA probe modified electrode were obtained in 10 mM Tris-HCl (pH 7.4) buffer containing 50 μM $Ru(NH_3)_6^{3+}$. It was employed to quantify the surface density of the duplex DNA probe immobilized on the electrode surface. Before electrochemical measurement, the electrolyte solution should be purged with high purity nitrogen for at least 20 minutes to avoid possible oxygen interference.

Results and Discussion

Fabrication principle of designed aptasensor

In this paper, we designed a simple and novel electrochemical aptasensor based on a responsive surface bioaffinity binding strategy, as illustrated in Scheme 1. The adenosine 5'-triphosphate (ATP) was used as a first model target. ATP has been well known as an energy storage molecule to play an important role in regulation of cellular metabolism and biochemical pathways.[41] A hairpin-like nucleic acid probe (HP) was designed with the aptamer sequence (red color) partially caged in the stem region by the complementary DNA sequences (black color). The residual aptamer sequence at the protruding 5'-terminus then hybridized with an immobilized probe strand (IP) to form a duplex DNA probe. The IP strand was dually labelled with sulfydryl and digoxigenin (Dig) at 3' and 5'-termini, respectively. The formed duplex DNA probe was then immobilized on the electrode surface via the Au-S interaction. The Dig was used as an affinity tag for the enzyme binding. Initially, the densely packed duplex DNA probe could shield the Dig from being approached by a bulky horseradish peroxidase linked-anti-Dig antibody (anti-Dig-HRP) due to the steric effect. In the absence of target only a low background current could be observed. After target binding with aptamer sequence, the HP probe undergoes a conformational change and dissociates from the IP strand.

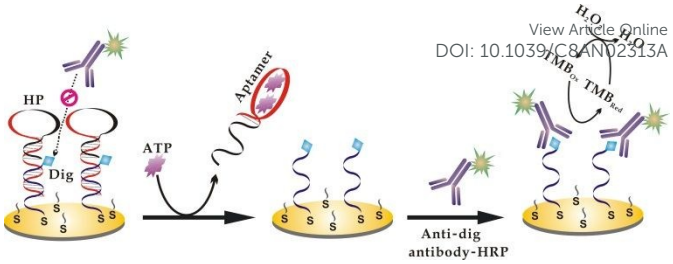

Scheme 1. Schematic illustration of electrochemical aptasensor fabrication principle.

Then the Dig was exposed to be accessible by the anti-Dig-HRP. The bound HRP could catalyze thousands of reduction reactions of H_2O_2, in the presence of TMB as a cosubstrate and electron shuttle, leading to the significantly amplified electrochemical signals related with target recognition event.[42,43] In current strategy, the target recognition and signal reporting units was relatively isolated, which made the design of aptasensor more simple, flexible and universal. It thus provided a direct and amplified avenue for target determination based on a responsive surface bioaffinity binding strategy.

Detection feasibility of fabricated aptasensor for ATP

The detection feasibility toward ATP of this proposed strategy was first tested. We have used cyclic voltammetry (CV) to investigate the electron transfer activity of TMB at the modified electrode surface. Two pairs of well-defined redox peaks ascribed to the two-electron reduction and oxidation of TMB could be observed at bare electrode in TMB and H_2O_2 solution (Figure S1). When the electrode was modified by duplex DNA probe, in the presence of ATP, a typical electrocatalytic behavior could be observed with a pair of asymmetric redox peaks of TMB and an apparently increased reduction peak at about 240 mV (curve b in Figure 1A), indicating the binding of anti-Dig-HRP on the electrode after ATP recognition for the occurrence of electrocatalysis. Herein, TMB served as an electron shuttle that could diffuse in and out of the redox site of the HRP, which coupled the catalytic reduction of H_2O_2 and resulted in the observed electrocatalytic peaks. The observed small shoulder peak at the reduction potential of about 0.22V might be caused by the electrochemical process of the adsorbed small amount of TMB on the DNA skeleton. As a comparison, only a small catalytic reduction peak of TMB could be found in the absence of ATP (curve a in Figure 1A), indicating that the immobilized duplex DNA probe could effectively shield the approaching of anti-Dig-HRP to the coupled Dig on the electrode. Also, we conducted the control experiment by using duplex DNA probe (no Dig label) modified electrode. The electrochemical responses of TMB were comparable with that at bare electrode and the catalytic response toward TMB could not be easily discernable in this case (curve c in Figure 1A). Since the IP strand modified electrode could be obtained after ATP recognition and HP dissociation, we also directly used the IP strand only immobilized electrode to mimic the recognized electrode. As expected, the IP strand only immobilized electrode showed a

View Article Online
DOI: 10.1039/C8AN02157A

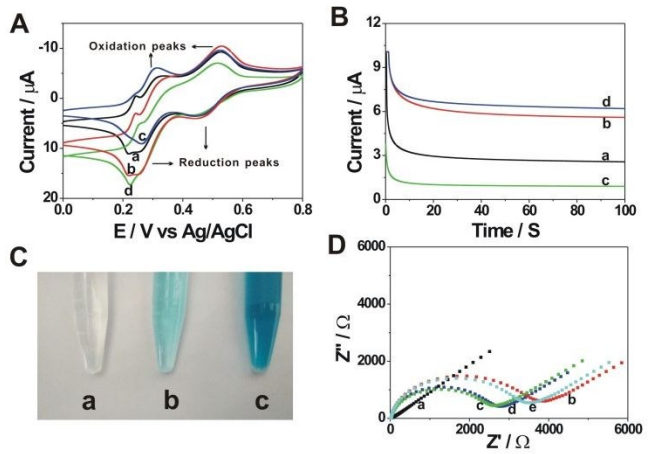

Figure 1. (A) CVs of duplex DNA probe modified electrode toward 0 (a) and 10 μM ATP (b) in TMB substrate. The curve (c) and (d) were obtained as control experiments by using duplex DNA probe (no Dig label) and IP strand only modified electrodes, respectively. Scan rate: 100 mV/s. (B) Amperometric curves obtained at corresponding experimental conditions that were the same with that of (A). Applied potential was 0.15 V. (C) The photograph of reaction system after immersion of different electrodes into TMB substrate. (D) Electrochemical impedance spectroscopy of bare electrode (a), duplex DNA probe modified electrode (b), ATP-treated electrode (c), after BSA blocking (d) and affinity binding with anti-Dig-HRP (e). In these experiments, the hairpin-like aptamer probe (HP-4, 20-base loop sequence) was used for the preparation of duplex DNA probe.

distinct catalytic reduction peak of TMB (curve d in Figure 1A). The CV experiments demonstrated the detection capacity of fabricated aptasensor toward ATP. Then, we used amperometry method to directly characterize the HRP catalyzed electrochemical process. A decay curve for the I-t relationship was recorded after the onset of the potential (0.15 V). As shown in Figure 1B, the steady-state electrochemical reduction current response could be obtained within 100 s. The steady current responses obtained in the I-t curves were related with the electrocatalytic reduction responses of TMB in CV curves. The ATP addition could induce a distinctly increased amperometric current (curve b in Figure 1B) than that of no ATP (curve a in Figure 1B). Also, the control experiments by using duplex DNA probe (no Dig label) or IP strand only modified electrodes showed the expected less or larger current responses, respectively (curves c and d in Figure 1B). Thus, the amperometric response trends obtained at different conditions (Figure 1B) were in basic accordance with the CV results (Figure 1A). At the same time, the testing solution color after immersion of treated electrodes could be followed with the naked eye (Figure 1C). The original testing solution of TMB and H_2O_2 is basically colorless (image a in Figure 1C). After ATP recognition and further incubation with anti-Dig-HRP, the anti-Dig-HRP was effectively conjugated on the electrode. Then the electrode was immersed into the testing solution and the conjugated HRP on the electrode could catalyze the oxidation of TMB in the presence of H_2O_2. The TMB was transformed into a blue oxidation product of cation radical.[44-46] Thus, a blue color could be observed for the testing solution (image c in Figure 1C). The color change of the testing solution also indicated that the anti-Dig-HRP had been effectively conjugated on the electrode by the interaction with the exposed Dig after ATP recognition for the catalyzed oxidation toward TMB.[47] In the absence of ATP, the anti-Dig-HRP could not be effectively conjugated on the electrode. Thus only a light blue color could be seen after the immersion of the electrode into the testing solution (image b in Figure 1C). The emerging background response could be attributed to the existed small amount of anti-Dig-HRP that escaped from the shielding effect owing to the inhomogeneity of modified electrode or non-specific adsorption. The whole aptasensor fabrication process was also followed with electrochemical impedance spectroscopy (EIS) method and shown in Figure 1D. EIS is an effective technique to characterize the conductivity of the electrode surface with the use of $[Fe(CN)_6]^{3-/4-}$ in the solution as a classical redox probe. The diffusion and charge transfer ability of this redox probe toward electrode surface for impedance information could well reflect the stepwise biosensor fabrication process. The semi-circle diameter in EIS diagram at higher frequencies corresponds to the charge-transfer resistance (Rct), and the linear part at lower frequencies is related to the diffusion process. The bare gold electrode presented an almost straight line and only a very small semi-circle with the Rct of about 15 Ω, revealing a diffusion-controlled electrochemical process (curve a in Figure 1D). Following with the sequential assembly of duplex DNA probe and MCH on electrode surface, an increased Rct value of about 3848 Ω were obtained (curve b in Figure 1D), indicating a distinct inhibition of $[Fe(CN)_6]^{3-/4-}$ diffusion by the immobilized insulating DNA and MCH monolayer. After ATP reaction, an evidently decreased Rct value of about 2612 Ω was observed (curve c in Figure 1D), which could be easily understood that the ATP binding with aptamer sequence dissociated the HP from the electrode surface, making the diffusion of $[Fe(CN)_6]^{3-/4-}$ relatively easy. The further treatment of BSA induced only a very slight increase of Rct value (curve d in Figure 1D). Then, the incubation of obtained electrode with anti-Dig-HRP induced an evident increase of Rct with the value of about 3520 Ω (curve e in Figure 1D), indicating that the effective binding with bulky anti-Dig-HRP offered an increased diffusion inhibition of $[Fe(CN)_6]^{3-/4-}$ toward electrode surface. The results of the EIS experiments further support the current strategy for aptasensor fabrication.

Optimization of experimental conditions

Herein, high-quality assembly of duplex DNA probe would benefit to shield the accessing of anti-Dig-HRP to the coupled Dig on the electrode for background inhibition. Thus, the assembly density of duplex DNA probe on the electrode surface was first optimized. It could be seen from Figure 2A that the background response decreased with the increasing immobilization concentration of duplex DNA probe and almost reached the minimum value at 5 μM of duplex DNA probe. The further increase of immobilization concentration to 10 μM caused no further evident suppression of background signal. It could be understood that the increased immobilization concentration induced a more densely packed assembly of duplex DNA probe on the electrode, offering the raised steric hindrance to inhibit the approaching of anti-Dig-HRP to the Dig

View Article Online
DOI: 10.1039/C9AN02437A

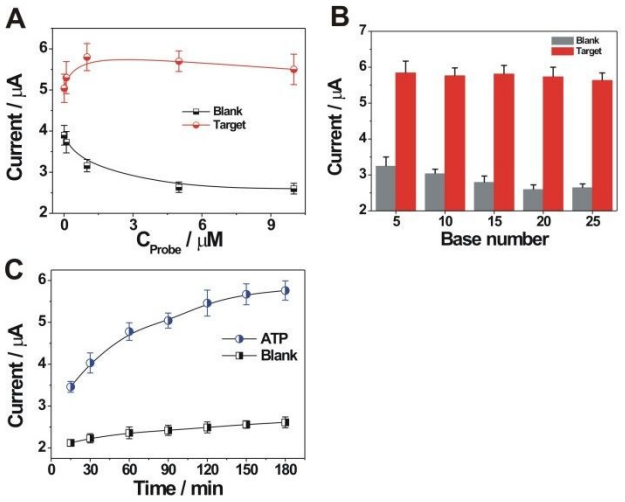

Figure 2. (A) Optimization of immobilization concentration of duplex DNA probe. The used immobilization concentrations were 0.01, 0.1, 1, 5, and 10 μM. (B) Base number optimization of loop sequence of HP. Different HPs (HP-1 to HP-5) with the loop sequences of 5, 10, 15, 20 and 25-base were employed. (C) Current responses of aptasensor with incubation time in the absence and presence of ATP. Reaction time: 15, 30, 60, 90, 120, 150 and 180 min. The used ATP concentration in (A), (B) and (C) was 10 μM. In (A) and (C), the HP-4 (20-base loop sequence) was employed for the preparation of duplex DNA probe.

for the decreased background signal. The surface density of duplex DNA probe could be calculated by chronocoulometry method with the use of $Ru(NH_3)_6^{3+}$ as a redox indicator.[48] The typical chronocoulometry curve of the immobilized duplex DNA probe was shown in Figure S2. The surface density of duplex DNA probe on the electrode surface at the immobilization concentration of 0.01, 0.1, 1, 5, 10 μM were calculated as about 6.21×10^{11}, 1.24×10^{12}, 2.77×10^{12}, 3.66×10^{12}, 4.1×10^{12} molecules/cm^2, respectively, indicating an increased assembly density of DNA monolayer. Also, the signal response increased with the immobilization concentration and almost reached the maximum value after 1 μM. Thus, considering background suppression and signal gain, 5 μM of duplex DNA probe was used as the optimized immobilization concentration. The surface density of 3.66×10^{12} molecules/cm^2 at 5 μM duplex DNA probe was converted to the average intermolecular spacing of 5.8 nm, which was far smaller than the size of anti-Dig-HRP (> 10 nm).[49,50] It thus provides sufficient steric hindrance to inhibit the approaching of anti-Dig-HRP to the anchored Dig. In current strategy, the base number of loop region in HP would also exert some effects on the background inhibition and then on the detection performance. A longer loop sequence is beneficial for preventing the anti-Dig-HRP from approaching the Dig owing to the extra steric hindrance effect induced by loop region, contributing a lower background response. We then investigated the effect of base number of HP loop on background and signal responses by using different loop sequences (5, 10, 15, 20, and 25-base). The results were shown in Figure 2B. It could be seen that the increased loop sequence length could reduce the background response to some extent. A loop sequence with 20-base basically showed a minimum background response in current system. Thus, the loop sequence with 20-base was enough for aptasensor fabrication. It should be noted that these duplex DNA probes with different lengths of loop sequence caused no evident change on surface density (data no shown). Thus the surface density of the duplex DNA probe was more influenced by the immobilization condition for example concentration and time but not the adopted loop sequence length. However, a longer loop sequence at the same surface density might cover a larger space and thus the loop region of the duplex DNA probe might be closer to each other. This brought some extra steric hindrance to inhibit the approaching of anti-Dig-HPR toward the confined Dig label on the stem region of the duplex DNA probe for the decreased background response. The target response time was also investigated (Figure 2C). It could be found that the background response was nearly invariable in the studied incubation time range. The target response signal increased with the reaction time and slowed down after 2 h. A plateau value could be obtained after 3h. Thus, the reaction time was determined as 3 h.

Detection performance of aptasensor for ATP

As revealed in Figure 3A, the steady current was highly dependent on ATP concentration and increased gradually as the ATP concentration increased from 0 to 100 μM. A linear response could be obtained between steady current and logarithm value of ATP concentration ranged from 1 nM to 10 μM (Figure 3B). The linear function was expressed as I (μA) = 9.428 + 0.712 log C_{ATP} (M) (R=0.9948) with a detection limit of 0.87 nM (S/N=3). Such a detection limit was much lower than many reported electrochemical methods (Table S2). The corresponding detection performances toward ATP and the following thrombin were also summarized in Table S3. The selective detection of the aptasensor to ATP was investigated by separately using other analogues such as TTP, CTP, GTP or NTP (the mixture of the same concentration of ATP, GTP, CTP

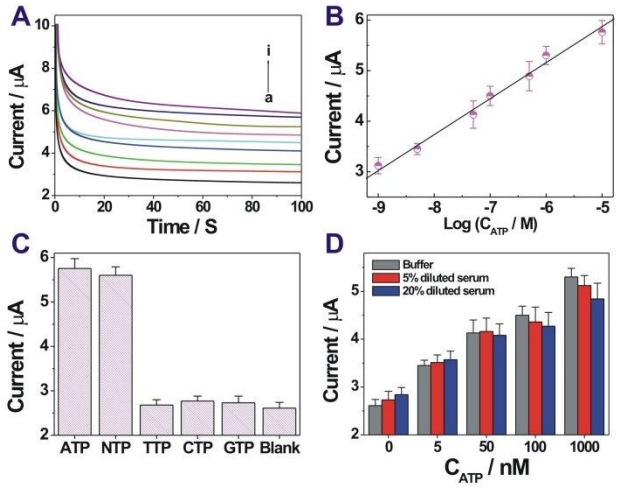

Figure 3. (A) Amperometric measurements for the detection of ATP with different concentrations (from a to i: 0, 1, 5, 50, 100 nM, 0.5, 1, 10 and 100 μM). (B) Relationship of steady currents versus logarithm value of ATP concentration. (C) Selective tests toward different solutions of blank, GTP, CTP, TTP, ATP and NTP mixture. Solution concentrations for ATP and different analogues were 10 μM. (D) Steady current responses toward the spiked ATP in buffer, 5% and 20% diluted serum. In these experiments, the hairpin-like aptamer probe (HP-4) was used for the ATP detection.

and GTP) as ATP substitute (all the concentrations for each analogue were 10 μM). The corresponding biosensor fabrication and detection processes toward each analogue were the same with that for ATP. As demonstrated in Figure 3C, the steady current caused by all three analogues were only comparable with the background responses, while the ATP and NTP mixture sample could give the obvious steady current responses. This confirmed that the proposed aptasensor had an excellent selectivity for ATP analysis. Also, we applied the fabricated aptasensors on a relatively complex sample matrix such as a diluted serum (Figure 3D). The serum could exert some influences on the background and signal responses. But the current responses were still dependent on the spiked ATP concentration in diluted serum. Thus, the developed aptasensors can be used even in relatively complex matrices.

The reproducibility of the duplex DNA probe modified electrode was also checked. The relative standard deviation for the detection of 0.1 μM ATP by using five different aptasensors fabricated on the same electrode was 3.94%, and it was 4.67% on five different electrodes. Furthermore, the long-term storage stability of constructed aptasensor was examined. The current intensity toward 0.1 μM ATP decreased less than 10% after the aptasensor was kept at 4 °C for two weeks. These results demonstrated the satisfactory reproducibility and stability of the developed aptasensor.

Generality of the proposed strategy for the detection of protein

The proposed strategy was also used for protein detection with the use of thrombin as a model analyte of interest. The design principle was the same with that of ATP except that the aptamer sequence for thrombin and the corresponding IP strand were re-designed. The used experimental conditions for thrombin detection were also referred with that of ATP. Cyclic voltammetry experiment showed a typical catalytic curve in the presence of thrombin (curve b in Figure 4A), and also the catalytic reduction peak current was evidently larger than that of no thrombin (curve a in Figure 4A). This indicated the detection capacity toward thrombin. The amperometric curves obtained at different concentrations of thrombin were shown in Figure 4B. As thrombin concentration increased, the corresponding steady current also increased and a linear plot could be obtained versus the logarithm value of thrombin concentration from 10 pM to 100 nM. The linear regression equation was obtained as I (μA) =10.0017 + 0.6103 log $C_{thrombin}$ (M) with a regression coefficient of 0.9931 (Figure 4C). A low detection limit of thrombin was obtained as 6.3 pM (S/N=3). Such a thrombin detection limit was comparable or superior to that of some reported electrochemical methods (Table S4). The selective detection toward thrombin was also studied by separately using other non-specific proteins as thrombin substitute (Figure 4D). Only thrombin gave an evident current response while other nonspecific proteins (BSA, IgG and streptavidin) could only exhibit the comparable responses with the background value. The detection of protein in diluted serum was also conducted to verify its applications in relatively complex samples. The serum is a recognized complex

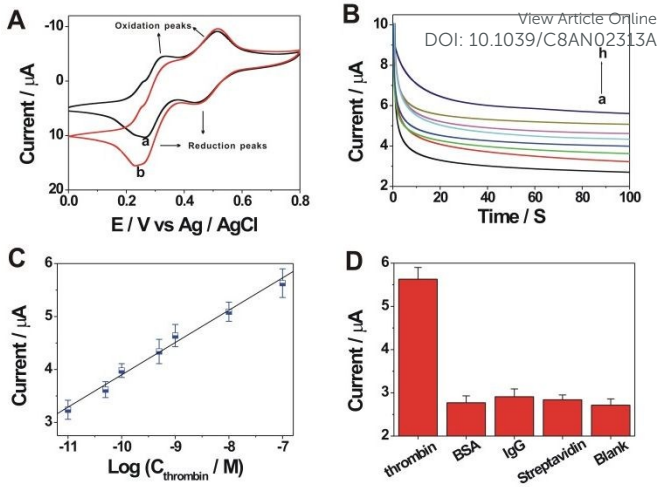

Figure 4. (A) CVs of the redox reaction of TMB substrate in the absence (a) and presence (b) of 100 nM thrombin. (B) Amperometric measurements for the detection of thrombin with different concentrations (from a to h: 0, 10, 50 100 pM, 0.5, 1, 10 and 100 nM). (C) Relationship of steady current responses versus logarithm value of thrombin concentration. (D) Selectivity tests toward thrombin and other non-specific proteins (all proteins have the same concentration of 100 nM).

biological matrix which contains a variety of proteins, enzymes, ions, etc. These interfering components might affect the thrombin recognition with its aptamer sequence and the further binding of anti-Dig-HRP with the Dig on the electrode. As shown in Figure S3, such interference could be more clearly seen especially at the higher thrombin concentrations (0.5 and 10 nM) and the relatively lower current responses in the diluted serum could be obtained than that in the buffer. Overall, the current responses for the spiked thrombin in diluted serum were basically comparable with that in buffer solution, showing its applications in relatively complex sample.

Conclusions

In summary, a new responsive surface bioaffinity binding strategy was well developed for sensitive electrochemical aptasensor fabrication with the use of ATP and thrombin as model targets. It took full advantages of the immobilized complex duplex probe to effectively inhibit the approaching of bulky anti-Dig-HRP to the Dig, and target recognition-induced the dissociation of aptamer strand with the exposed Dig for enzyme binding. The successive electrocatalysis induced significantly amplified electrochemical signals related with target recognition event. Sensitive detection toward ATP and thrombin was achieved with detection limits of 0.87 nM and 6.3 pM, respectively. The proposed strategy is very simple without complex operation that confronts many amplified aptasensors. Also the target recognition and signal reporting units in current system are relatively separated, which make the biosensor fabrication more flexible and universal. It would be easily applied for the analysis of a wide spectrum of targets such as small molecules, proteins and nucleic acids, and thus hold a promising potential for the application in bioanalysis and disease diagnostics.

Conflicts of interest

There are no conflicts to declare

Acknowledgements

We appreciated the finance supports from the National Natural Science Foundation of China (21475072), the Natural Science Foundation of Shandong Province of China (JQ201704), the Key Research and Development Program of Shandong Province of China (2016GSF201208 and 2018GGX102001), and the Open Project from Fujian Provincial Key Laboratory of Ecology-Toxicological Effects & Control for Emerging contaminants.

Notes and references

1 A. D. Ellington and J. W. Szostak, *Nature*, 1990, **346**, 818.
2 C. Tuerk and L. Gold, *Science*, 1990, **249**, 505.
3 S. Jhaveri, M. Rajendran and A. D. Ellington, *Nat. Biotechnol.*, 2000, **18**, 1293.
4 W. Zhou, P. J. J. Huang, J. Ding and J. Liu, *Analyst*, 2014, **139**, 2627.
5 A. B. Iliuk, L. Hu and W. A. Tao, *Anal. Chem.*, 2011, **83**, 4440.
6 Y. Jiang, M. Shi, Y. Liu, S. Wan, C. Cui, L. Zhang and W. Tan, *Angew. Chem. Int. Ed.*, 2017, **56**, 11916.
7 Z. Tang, D. Shangguan, K. Wang, H. Shi, K. Sefah, P. Mallikratchy, H. W. Chen, Y. Li and W. Tan, *Anal. Chem.*, 2007, **79**, 4900.
8 S. Y. Toh, M. Citartan, S. C. B. Gopinath and T. H. Tang, *Biosens. Bioelectron.*, 2015, **64**, 392.
9 X. Fang and W. Tan, *Acc. Chem. Res.*, 2010, **43**, 48.
10 M. Liss, B. Petersen, H. Wolf and E. Prohaska, *Anal. Chem.*, 2002, **74**, 4488.
11 T. A. Feagin, N. Maganzini and H. T. Soh, *ACS Sens.*, 2018, **3**, 1611.
12 W. W. Zhao, J. J. Xu and H. Y. Chen, *Trac-Trend. Anal. Chem.*, 2016, **82**, 307.
13 L. Wang, L. Fang and S. Liu, *Analyst*, 2015, **140**, 5877.
14 H. Zhang, L. Zhou, Z. Zhu and C. Yang, *Chem. Eur. J.*, 2016, **22**, 9886.
15 Y. Wu, F. Xiao, Z. Wu and R. Yu, *Anal. Chem.*, 2017, **89**, 2852.
16 S. Rauf, L. Zhang, A. Ali, Y. Liu and J. Li, *ACS Sens.*, 2017, **2**, 227.
17 I. Willner and M. Zayats, *Angew. Chem. Int. Ed.*, 2007, **46**, 6408.
18 H. Li, N. Arroyo-Currás, D. Kang, F. Ricci and K. W. Plaxco, *J. Am. Chem. Soc.*, 2016, **138**, 15809.
19 H. Li, P. Dauphin-Ducharme, N. Arroyo-Currás, C. H. Tran, P. A. Vieira, S. Li, C. Shin, J. Somerson, T. E. Kippin and K. W. Plaxco, *Angew. Chem. Int. Ed.*, 2017, **56**, 7492.
20 M. Labib, E. H. Sargent and S. O. Kelley, *Chem. Rev.*, 2016, **116**, 9001.
21 L. Wu, X. Zhang, W. Liu, E. Xiong and J. Chen, *Anal. Chem.*, 2013, **85**, 8397.
22 R. J. White, N. Phares, A. A. Lubin, Y. Xiao and K. W. Plaxco, *Langmuir*, 2008, **24**, 10513.
23 X. Zhang, C. Song, K. Yang, W. Hong, Y. Lu, P. Yu and L. Mao, *Anal. Chem.*, 2018, **90**, 4968.
24 X. Zuo, S. Song, J. Zhang, D. Pan, L. Wang and C. Fan, *J. Am. Chem. Soc.*, 2007, **129**, 1042.
25 Y. Lu, X. Li, L. Zhang, P. Yu, L. Su and L. Mao, *Anal. Chem.*, 2008, **80**, 1883.
26 J. A. Hansen, J. Wang, A. Kawde, Y. Xiang, K. V. Gothelf and G. Collins, *J. Am. Chem. Soc.*, 2006, **128**, 2228.
27 T. Zhao, R. Liu, X. Ding, J. Zhao, H. Yu, L. Wang, Q. Xu, X. Wang, X. Lou, M. He and Y. Xiao, *Anal. Chem.*, 2015, **87**, 7712.
28 R. Polsky, R. Gill, L. Kaganovsky and I. Willner, *Anal. Chem.*, 2006, **78**, 2268.
29 S. Su, H. Sun, W. Cao, J. Chao, H. Peng, X. Zuo, L. Yuwen, C. Fan and L. Wang, *ACS Appl. Mater. Interfaces*, 2016, **8**, 6826.
30 W. Li, Z. Nie, X. Xu, Q. Shen, C. Deng, J. Chen and S. Yao, *Talanta,* 2009, **78**, 954.
31 S. Liu, Y. Wang, C. Zhang, Y. Lin and F. Li, *Chem. Commun.*, 2013, **49**, 2335.
32 T. Hu, W. Wen, X. Zhang and S. Wang, *Analyst,* 2016, **141**, 1506.
33 D. Zhang, F. Ma, Q. Zhang and C. Y. Zhang, *Chem. Commun.*, 2017, **53**, 11496.
34 J. Yang, B. Dou, R. Yuan and Y. Xiang, *Anal. Chem.*, 2017, **89**, 5138.
35 Y. Ji, L. Zhang, L. Zhu, J. Lei, J. Wu and H. Ju, *Biosens. Bioelectron.,* 2017, **96**, 201.
36 S. S. Mahshid, A. Vallée-Bélisle and S. O. Kelley, *Anal. Chem.*, 2017, **89**, 9751.
37 G. Liu, Y. Wan, V. Gau, J. Zhang, L. Wang, S. Song and C. Fan, *J. Am. Chem. Soc.,* 2008, **130**, 6820.
38 B. Jiang, M. Yang, C. Yang, Y. Xiang and R. Yuan, *Sensors and Actuators B*, 2017, **247**, 573.
39 M. J. O'Donnell, K. Tang, H. Köster, C. L. Smith and C. R. Cantor, *Anal. Chem.*, 1997, **69**, 2438.
40 T. M. Herne and M. J. Tarlov, *J. Am. Chem. Soc.*, 1997, **119**, 8916.
41 A. V. Gourine, E. Llaudet, N. Dale and K. M. Spyer, *Nature*, 2005, **436**, 108.
42 C. Li, D. Wu, X. Hu, Y. Xiang, Y. Shu and G. Li, *Anal. Chem.*, 2016, **88**, 7583.
43 Y. Wen, H. Pei, Y. Wan, Y. Su, Q. Huang, S. Song and C. Fan, *Anal. Chem.*, 2011, **83**, 7418.
44 P. D. Josephy, T. Eling and R. P. Mason, *J. Biol. Chem.*, 1982, **257**, 3669.
45 L. S. A. Busa, M. Maeki, A. Ishida, H. Tani and M. Tokeshi, *Sensors and Actuators B*, 2016, **236**, 433.
46 L. Cui, J. Wu, J. Li and H. Ju, *Anal. Chem.*, 2015, **87**, 10635.
47 J. Chen, J. Zhang, Y. Guo, J. Li, F. Fu, H. H. Yang and G. Chen, *Chem. Commun.*, 2011, **47**, 8004.
48 A. B. Steel, T. M. Herne and M. J. Tarlov, *Anal. Chem.*, 1998, **70**, 4670.
49 S. S. Mahshid, S. Camiré, F. Ricci and A. Vallée-Bélisle, *J. Am. Chem. Soc.*, 2015, **137**, 15596.
50 J. Zhu, H. Gan, J. Wu and H. Ju, *Anal. Chem.*, 2018, **90**, 5503.

View Article Online
DOI: 10.1039/C8AN02313A

Table of Contents

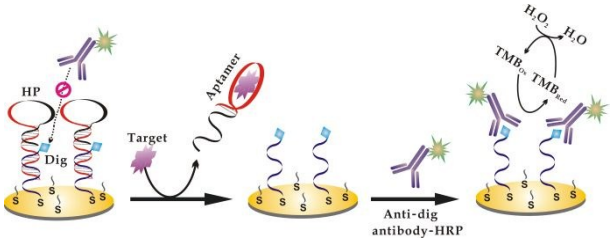

A responsive surface bioaffinity binding strategy was developed for fabrication of simple, flexible and amplified electrochemical aptasensor